Monte Carlo simulations concerning elastic scattering with application to DC and high power pulsed magnetron sputtering for Ti_3SiC_2

Jürgen Geiser and Sven Blankenburg

Humboldt-Universität zu Berlin,
Department of Mathematics,
Unter den Linden 6, D-10099 Berlin, Germany
geiser@mathematik.hu-berlin.de
sven.blankenburg@physik.hu-berlin.de

Abstract. We motivate our study by simulating the particle transport of a thin film deposition process done by PVD (physical vapor deposition) processes. In the paper we present several collision models for projectile and target collisions in order to compute the mean free path and the differential cross section (angular distribution of scattered projectiles) of the scattering process. The detailed description of collision models is of highest importance in Monte Carlo Simulations of high power impulse magnetron sputtering and DC sputtering. We derive an equation for the mean free path for arbitrary interactions (cross sections) that include the relative velocity between the particles. We apply our results to two major interaction models: hard sphere interaction & Screened Coulomb interaction. Both types of interaction separates DC sputtering from HIPPIMS. Further investigations presented in this paper involve modifications of the scattering angle probability distribution due to initially moving background targets. In order to tackle this modification, an appropriate Monte-Carlo-Markov-Chain approach is proposed.

Keywords: DC sputtering, High power pulsed magnetron sputtering,MAX-phases, mean free path, scattering angle probability distribution, moving targets, Particle-In-Cell-Monte-Carlo-Collisions (PIC-MCC), Monte-Carlo-Markov-Chain.
AMS subject classifications. 80M31, 60J20, 65N74, 65C05, 65C35, 65C40

We motivate our studying on simulating thin film deposition processes that can be done by sputtering processes, see [2]. In the last years, the research in producing high temperature films by depositing of low pressure processes have increased. Due to standard applications in deposing TiN and TiC, that are immense, recently also deposition with new material classes known as MAX-phases became be more and more important. The MAX-phase are nanolayered terniar metal-carbides or -nitrids, where M is a transition metal, A is an A-group element (e.g. Al, Ga, In, Si, etc.) and X is C (carbon) or N (nitrid). We

present a particle tracking model for low temperature and low pressure plasma. The aim of the first part is to check an easy model for the particle dynamics within a magnetron sputtering process, which is ultimately designed in order to create thin films of so-called MAX-phases at the workpiece. In this model a purely Monte Carlo dominated approach is presented and some numerical results are given. In the next part, the model is extended with respect to the pathway model, see [7], to achieve the parameters of the model obtain the deposition rates of the stoichiometry $3Ti$, Si and $2C$.

This paper is outlined as follows: In Section 1 we define the reasons for our investigation on the scattering process of hard spheres and Coulomb interactions. In Section 2 we describe the concept of mean free path and derive on the basis of kinetic theory an appropriate expression for the mean free path of an external particle (projectile) that is probing into an ensemble of target particles, which constitute an ideal gas (background gas). The main modification to standard mean free paths is the implementation of initially moving targets. Subsequently in Section 3 we study from first principles the concept of differential cross section and perform again a modification of standard formulae to obtain a realistic scattering angle probability distribution for the projectiles, which respects initially moving targets. In 4 we present our Monte Carlo Method based on a Pathway model[7] and perform several simulations to direct current (DC) and high power pulsed magnetron sputtering (HIPPIMS). At the end in Section 5 we summarize our results and show an outlook to our future work.

1 Motivation

The main reason for studying in detail the collision processes of elastic scattering is the need for a reliable physical description of interactions between ions and a plasma (background gas) in high power impulse magnetron sputtering processes in order to create thin films by plasma techniques. The MAX phases experienced a renaissance in the mid-1990s, when Barsoum synthesized relatively phase-pure samples of the MAX phase Ti_3SiC_2, and discovered a material with a unique combination of metallic and ceramic properties: it exhibited high electrical and thermal conductivity, and it was extremely resistant to oxidation and thermal shock, which makes them very attractive for industrial applications like proton exchange fuel cells (PEFC). These stoichiometries (MAX phases) are described by a general formula: $M_{n+1}AX_n$, whereby M is an early transition metal (Se, Ti, V, Cr, Zr, Nb, Mo, Hf, Ta), A is an A-group element (Al, Si, P, S, Ga, Ge, As, Cd, In, Sn, Ti, Pb), and X is either Carbon and/or Nitrogen. The different MAX stoichiometries are often referred to as 211 ($n = 1$), 312 ($n = 2$). Recent developments has led to a new method to evaporate thin films of MAX-phases at a substrate (workpiece): high power impulse magnetron sputtering (HIPIMS or HPPMS). The most important ingredient in sputtering processes is a plasma, i.e. a partially ionized gas, which is electrically neutral at macroscopic scales. If any material body like a substrate is immersed into a plasma it will acquire a potential slightly negative with respect to ground. This effect is known as floating

potential. The physical reason for this is the higher mobility of electrons than that of ions. Hence, more electrons reach the substrate surface than ions. The most sensitive quantity in sputtering processes (with respect to the experimental setup: gas-pressure, temperature, target-material, etc.) is the sputtering yield, which describes the ratio of atoms ejected from a target surface per incident ion. The sputtering yield can take almost any value from 0.1 up to 10. For reasons of optimized production, one is generally interested in obtaining as high values for the sputtering yield as possible. In order to obtain a well defined stoichiometric at the substrate, one has to take transport mechanism of the sputtered particles within the plasma into account. This can be done within a macroscopic description of the transport phenomena, i.e. solution of the advection-diffusion equation, or at a microscopic scale, via Monte-Carlo simulations of the transport phenomena. This paper deals almost exclusively with the last approach, whereby the ultimate goal of our work will be in future to link both approaches to each other (this will be presented in future papers).

2 Collision Model : mean free path

The mean free path or average distance between collisions for a gas molecule may be estimated from kinetic theory. If one assumes the gas be consisted of hard spheres (non overlapping spheres), then the effective collision area is given by

$$\sigma = \pi \left(d_1 + d_2\right)^2 = \pi D^2. \tag{1}$$

In time δt, the area sweep out the volume $V_{interaction}$ and the number of collisions can be estimated from the number of target molecules (n_V) that are in that volume.

$$V_{interaction} = \sigma v \delta t. \tag{2}$$

$$\lambda = \frac{|v_{proj}|\delta t}{V_{interaction} n_V} = \frac{|v_{proj}|\delta t}{\pi D^2 v \delta t n_V} = \frac{1}{\pi D^2 n_V} \tag{3}$$

This expression for the mean free path is a good approximation, but it suffers from a significant flaw - it assumes the target objects being at rest, which is of course physically nonsense. By introducing an relative velocity between the gas objects

$$v_{rel} = \sqrt{2} v. \tag{4}$$

Whereby the $\sqrt{2}$ results from the molecular speed distribution of a mono atomic ideal gas (Maxwell Boltzmann distribution). We therefore have the expression

$$\lambda = \frac{1}{\sqrt{2}\pi D^2 n_V}. \tag{5}$$

The number of molecules per unit volume can be determined from the state equation of the gas

$$pV = \left(1 + B_1 + B_2 + ...\right) RT. \tag{6}$$

If one assumes an ideal gas (non interaction and non overlapping gas particles) one can neglect the so called higher Virial coefficients ($B_1 + B_2 + ...$). Inserting the state equation for an ideal gas into 5, one gets

$$\lambda = \frac{(1)\, RT}{\sqrt{2}\pi D^2 N_A p}. \tag{7}$$

Whereby R is the gas constant and N_A is Avogadro's number. This is an approximation for mean free path for an atom/molecule of an ideal gas. In our problem however, we have to calculate the mean free path of an external particle (projectile) which is not a member of the background gas (ideal gas). This can be done by modifying the average relative velocity between projectile and target. This is done in the next part.

2.1 The mean relative velocity between projectiles and targets

The background gas is assumed to be Maxwell distributed in velocity (this is motivated by the assumption of an ideal gas). Because of the fact that the background particles being a particle ensemble (with statistically distributed velocities) one can just speak of a mean relative velocity $< |\boldsymbol{v_{rel}}| >=< |\boldsymbol{v_{proj}} - \boldsymbol{v_{target}}| >$, which can be calculated via:

$$< |\boldsymbol{v_{rel}}| >= \int\int\int_V |\boldsymbol{v_{proj}} - \boldsymbol{v_{target}}| Z(\boldsymbol{v_{target}}) d\boldsymbol{v_{target}}. \tag{8}$$

Where Z is the three-dimensional Maxwell distribution given by

$$Z(\boldsymbol{v_{target}}) = (A/\pi)^{3/2} \frac{1}{2\sqrt{2}} \exp\left(-A\boldsymbol{v_{target}}^2\right). \tag{9}$$

With the abbreviation $A = M_{target}/2k_BT$. A complete derivation of the solution can be found in the appendix. The result is

$$|\boldsymbol{v_{rel}}| = \frac{\left[\left(s + \frac{1}{2s}\right) \mathrm{erf}(s) + \frac{1}{\sqrt{\pi}} \exp\left(-s^2\right)\right]}{3s} \times |\boldsymbol{v_{proj}}|. \tag{10}$$

With $s = a\sqrt{A}$ (scalar) and $a = |v_{proj}|$. We now want to discuss a few special cases.
If the velocity of the projectile is very small $|v_{proj}| \approx 0$, then $s \approx 0$ and therefore the following approximation holds

$$v_{rel} \approx v_{target}. \tag{11}$$

This gives equation number 3 as expected.
If the targets objects are identical the projectile objects (same mass and same mean velocity), then the following limit holds

$$|v_{rel}| \approx 1.41 |v_{target}|, \tag{12}$$

which gives the factor $\sqrt{2} \approx 1.41$ and leads to the mean free path of an element of a mono atomic ideal gas (as expected). However, the general expression for the mean free path of a projectile probing into an ideal gas with pressure P_{gas} and temperature T is given by

$$\lambda_{proj} = \frac{3}{4\pi} \frac{s}{\left[\left(s + \frac{1}{2s}\right) \mathrm{erf}(s) + \frac{1}{\sqrt{\pi}} \exp\left(-s^2\right)\right]} \frac{k_B T}{\left(R_{ion} + R_{target}\right)^2 P_{gas}}. \tag{13}$$

There are a few things to say about this expression. First, the main assumption that the background gas (ensemble of target particles) is an ideal gas, is just valid within the high vacuum regime, i.e. small target density. Second, the interaction between the the projectile and target atoms are assumed of hard sphere type, i.e. purely geometric interaction. If the projectile is a free particle between the interactions, its Hamilton function reads

$$H = \frac{p^2}{2M_{proj}} = E. \tag{14}$$

In this case one can easily compute $a = |\boldsymbol{v_{proj}}| = \sqrt{\frac{2E}{M_{proj.}}}$. It follows immediately

$$s = a\sqrt{A} = \sqrt{\frac{E}{k_B T}} \sqrt{\frac{M_{target}}{M_{proj}}}. \tag{15}$$

In appropriate units (atomic units) the scalar s reads:

$$s = 107.7242 \sqrt{\frac{E[eV]}{T[K]}} \sqrt{\frac{M_{target}}{M_{proj}}}. \tag{16}$$

And therefore the mean free path in units of cm is given by:

$$\begin{aligned} \lambda_{proj}[cm] = & \frac{s}{\left[\left(s + \frac{1}{2s}\right) \mathrm{erf}(s) + \frac{1}{\sqrt{\pi}} \exp\left(-s^2\right)\right]} \\ & \times \frac{3.297\mathrm{cm} \cdot T[K]}{\left(R_{ion}[pm] + R_{target}[pm]\right)^2 P_{gas}[mbar]}. \end{aligned} \tag{17}$$

Eklund ([2]) used a formula for the mean free path of ions surrounded by an ideal gas of pressure p_{ar} given by

$$\lambda[cm] = \frac{4.39\mathrm{cm} \cdot T[K]}{\sqrt{\left(1 + \frac{M_{ion}}{M_{target}}\right)} \left(r_{ion}[pm] + r_{target}[pm]\right)^2 p_{target}[mbar]}. \tag{18}$$

The following table shows the mean free path for ions at $E = 3\mathrm{eV}$ and $T = 300\mathrm{K}$ and gas pressure $p = 4 * 10^{-3}$ mbar.

Ion	Eq. 17	Eq. 18
carbon (12)	12.96cm	15.18cm
silicon (28)	7.52cm	7.71cm
titanium (48)	5.03cm	4.55cm

In a sputtering process, the the ions obey a kinetic energy distribution as well as an angular-distribution at the target. Because of different transport mechanism, the ion looses some extend of their initial kinetic energy. An individual ion within a sputter process can therefore be classified into three groups. First, the **ballistic group**, which is excelled in the way that any member of the ballistic group travels from the target to the substrate in a straight line, because no collisions occur. The **transition group** is characterized by the observation that the path of the ion is not a straight line and therefore the ions of this group undergo some collisions but still retain some of their initial energy. The last group is the **thermalized or diffusive group**, whereby any member of this group is characterized by an complete loss of their initial kinetic energy. The motion of such an ion is therefore described by a random walk. The typical distances between the target and the substrate are of the order of $5 - 15$cm. Hence, at low argon pressures we can classify carbon as more or less ballistic, and silicon and titanium as transition or thermalized. One can also see that the formula used by Eklund (2007) ([2]) is quite a good approximation, although it lacks from an energy dependency of the mean free path with respect to the ion energy. There are several attempts to achieve an energy dependency in the mean free path. But most of them are more or less physical consistent. For example, Mahieu et al. (2006) [5] use a formula, whereby the energy dependency is arrived by modifying the naive mean free path by multiplying the naive formula with the ion energy. This is of course unphysical because it implies a zero mean free path at very low ion energies and consequently the associated cross section is infinite. We hope that our formula for the mean free path will positively accepted within the community and might help to implement a realistic description of the interactions between particles. In Fig. 1 one can see the results from Eq. 16 and 17 with respect to the ion energy E (kinetic energy) at an argon pressure of $p = 4 \cdot 10^{-3}$mbar and a constant temperature of $T = 700$K, whereby the following constants were used.

element	atomic mass [u]	atomic radius [pm]
Ar	39.948	71
C	12.0107	67
Si	28.0855	110
Ti	47.867	150

One can see that the mean free path decrease with increasing kinetic energy of the ion and that the mean free path is almost constant at energies above 2 eV. The likelihood of ions to scatter off argon targets is not constant. Because if the ions scatter off an target it looses some amount of energy and therefore its mean free path becomes smaller. This iterative procedure continue. It is therefore of highest

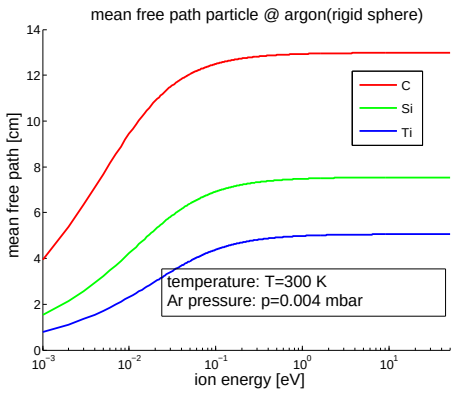

Fig. 1. mean free path of projectiles @ argon targets ($p = 4{*}10^{-3}$mbar and $T = 300$K).

importance in situations in which one has to deal with multiple scattering. this is the case if the sputter-target and the substrate are more than 4 cm removed.

3 Collision Model: differential cross section & angular distribution

With the help of the mean-free-path λ one is able within a Monte Carlo approach to determine collision frequency. But several questions are unsolved by the mean-free-path. If one is interested in a detailed description (kinematic) of the scattering process, one has to work out the differential cross section. We propose two descriptions, both are within their limits applicable. In the first model, we assume the target particle is initially at rest, whereby the second model will loose this restriction generally.

3.1 Scatter off initially fixed targets

If the projectile velocity is much higher than the target velocity one can assume the target atoms initially at rest. In describing the scattering process within the Center-of-Mass-System (CMS) of both particles one can simplify the calculations. The theoretical analysis of such a scattering process can be found in almost any text book on classical mechanics like [3]. We use spherical coordinates, whereby θ,ϕ describing the coordinates in the laboratory and Θ,Φ are the coordinates in the CMS. The ratio

$$\rho = \frac{M_{proj}}{M_{target}} \frac{v_{t,1}}{v_{rel,1}} \tag{19}$$

can be used to connect the scattering angles in the laboratory and the CMS (radial symmetric scattering potential)

$$\cos\theta = \frac{\cos\Theta + \rho}{\sqrt{1 + 2\rho\cos\Theta + \rho^2}}. \tag{20}$$

The transformation from CMS coordinates to laboratory coordinates commands the Jacobian as an extra factor:

$$\sigma(\theta) = \sigma(\Theta)\frac{\sin\Theta}{\sin\theta}\left|\frac{d(\Theta,\Phi)}{d(\theta,\phi)}\right|. \tag{21}$$

Because of $\Phi = \phi$ the Jacobian reduces to

$$\sigma(\theta) = \sigma(\Theta)\left|\frac{d\cos\Theta}{d\cos\theta}\right|. \tag{22}$$

With the help of Eq.20 one gets:

$$\sigma(\theta) = \sigma(\Theta)\frac{\left(1+2\rho\cos\Theta+\rho^2\right)^{3/2}}{1+\rho\cos\Theta}. \tag{23}$$

The energy transfer from projectile to target (elastic scattering) is given by:

$$\Delta E = \frac{E_{\text{proj,new}}}{E_{\text{proj,old}}} = \frac{1+2\rho\cos\Theta+\rho^2}{(1+\rho)^2}. \tag{24}$$

The differential cross section is however not exactly the scattering angle distribution, because we have to remember that the angular distribution is given by an extra factor of $\sin\theta$ followed by an integration over ϕ, i.e

$$\sigma_{total} = \int_0^{\pi} \underbrace{\int_0^{2\pi} \frac{\sin\theta\sigma(\theta)}{4\pi} d\phi}_{\text{probability distribution}} \; d\theta. \tag{25}$$

Hard sphere Collision In order to model the transport mechanism within a DC sputtering process, one recognizes experimentally that most of the background targets as well as the sputter particles are not ionized and therefore it seems absolutely reasonable that the interaction of both projectile and targets are purely geometric and can be modeled by a hard sphere interaction. The Scattering angle Θ_{CMS} in the Center-Of-Mass system of a binary collision can in generally be calculated for any given interaction potential $V(r)$ with the help of:

$$\begin{aligned}\Theta_{CMS} &= \pi - 2\int_{r_0}^{\infty} \left(r\phi(r)\right)^{-1} dr \\ \phi(r) &= \left(\frac{r^2}{p^2} - 1 - \frac{r^2 V(r)}{1/2\mu v_{rel}^2 p^2}\right)\end{aligned} \tag{26}$$

μ is the reduced mass in the CMS system, i.e. $\mu = \frac{M_1 M_2}{M_1+M_2}$ and v_{rel} the relative velocity of the scattering partner. p is called the impact parameter. In Fig. 2 one can see the scattering angle θ in the laboratory of several incident projectiles at argon atoms (held at rest) and the maximal scattering angle θ_{max} in the

laboratory with respect to the mass ratio ρ. In the case of a hard sphere potential, i.e.

$$V(r) = \begin{cases} \infty, & \text{for } r < R \\ 0. & \text{for } r \geq R \end{cases}, \tag{27}$$

the integral can be computed analytically and the result is:

$$\Theta_{CMS} = 2\cos^{-1}(z). \tag{28}$$

Whereby we have used the dimensionless parameter $z = p/p_{max} = p/R$ with $R = R_1 + R_2$ the radius of interaction. The impact parameter p is chosen to be uniformly distributed between 0 and p_{max}, i.e. $z \in U[0, 1]$. In Fig. 2 one can see the results from single binary collisions for the sputter species C,Si and Ti within the framework of hard sphere collisions. One can see, that as long as the projectile mass is smaller than the target mass all scattering angles are allowed. However, this changes if the mass ratio becomes greater than 1. In this case only a cone of scattering directions is allowed, whereby the opening angle of the cone decreases with increasing mass ratio. In the case of titanium projectiles at argon targets, only scattering angles between 0 and $\theta_{\max} \approx 60$ degrees are allowed. Titanium projectiles are therefore subjected to forward scattering and the cone angle is around 120 degrees. The above given approach is quite satisfactory if one assumes high energetic projectiles (with respect to target velocity) and the suppression of multi-scattering events. A proper description of the kinematic should include the random motion of the target projectiles and therefore an energy dependency for the differential cross section. The total cross section has to be unchanged, because the total area per target cannot depend on the relative velocity of the target and projectile, because the total cross section is an intrinsic quantity.

Screened Coulomb collision Now we want to investigate the kinematics of the scattering process whereby we assume a Coulomb like interaction between the sputter particles and the gas atoms (neglecting interactions between the sputter particles again). This is motivated by the experimentally fact, that in High power impulse Magnetron sputtering processes a fraction of the background gas as well as the sputtered particles are ionized and consequently the interaction model should include long range interaction due to electrical repulsion between both particles (ions). Our method of investigation is quite the same as in the the previous (hard sphere) collision model. First we will specify the interaction potential and after that we compute the scattering angle in the CMS system. With the help of the scattering angle in the CMS we can compute the scattering angle in the LAB frame and also the energy loss. We have chosen the following screened interaction potential

$$V(r) = \frac{Z_1 Z_2 k}{r} \exp(-r/a). \tag{29}$$

Whereby Z_1 and Z_2 are the atomic numbers of the collision partners, r is the radial distance between both partners, k is a constant ($k = 1.44$MeV fm) and a

is the screening length given by

$$a = \frac{a_0}{\sqrt{\left(\sqrt{Z_1} + \sqrt{Z_2}\right)}}. \tag{30}$$

With $a_0 = 0.53 \cdot 10^{-10} m$ the first Bohr radius of the hydrogen atom. For any given scattering potential, the scattering angle in the CMS system can be computed with the help of Eq. 26 . As we mentioned earlier in this paper, the integral can just be solved analytically with respect to the hard sphere interaction and a pure Coulomb interaction. However, we have chosen a screened Coulomb potential and we must therefore evaluate the integral numerically. In order to reduce round off errors we reformulate the integral (this procedure is motivated by [6]):

$$\Theta_{CMS} = 2\mathrm{Arccot}\left(\frac{2\chi_2}{\exp\left(-1/z_0\right)}\right) + 2\chi_0\chi_2 \int_0^{z_0} \left(y_0^{1/2}(z) - y^{1/2}(z)\right) dz. \tag{31}$$

Whereby we made us of:

$$\begin{aligned}
\chi_0 &:= \frac{b}{a} = \frac{Z_1 Z_2 \sqrt{\left(\sqrt{Z_1} + \sqrt{Z_2}\right)}}{E_{CMS}[\mathrm{eV}]} \cdot 27.17 \\
\chi_2 &:= \frac{p}{b} = \frac{p[10^{-10}\mathrm{m}] E_{CMS}[\mathrm{eV}]}{Z_1 Z_2} \cdot \frac{1}{14.4} \\
E_{CMS} &= \frac{\left((1 + 1/2s)\mathrm{erf}(s) + 1/\sqrt{\pi}\exp\left(-s^2\right)\right)^2}{\left(1 + \frac{M_{proj}}{M_{target}}\right) 9s^2} \cdot E_{proj} \\
y_0(z) &= 1 - \left(\chi_0\chi_2\right)^2 z^2 - \chi_0 z \exp\left(-1/z_0\right) \\
y(z) &= 1 - \left(\chi_0\chi_2\right)^2 z^2 - \chi_0 z \exp\left(-1/z\right) \\
z &= r/a
\end{aligned} \tag{32}$$

Our procedure is then as follows: for a given impact parameter p in units of fm we can solve the integral numerically for every sputtering species. Because is is very time consuming we have done this for several impact parameter and every species before the simulation and we have stored the results in a data file, which is used during the simulation. During the Monte Carlo simulation an impact parameter is chosen from a uniform distribution between zero and p_{max} whereby we have chosen $p_{max} = 4 \cdot 10^{-10}$m, because for impact parameter greater than p_{max} the scattering angle in the laboratory system is in general smaller than 0.1 degree. With the help of the numerical integration of Eq. 26 we can compute the scattering angle in the CMS and therefor compute the scattering angle in the laboratory system. Remind, that here we choose the impact parameter to be uniformly distributed in the CMS system and not the scattering angle (as we did in the hard sphere scattering). Remind also, that we have chosen our appropriate relative velocity between projectiles and targets (the derivation can be found in the appendix). In Figure 3 one can see the scattering angle of several species with respect to a screened Coulomb interaction potential. Again, all scattering angles

between zero and 180 degree are possible for projectiles with a mass smaller than the target mass. For projectiles with a mass greater than the target mass there exists a maximum scattering angle and therefore the scattering occurs only with an scattering cone of finite opening angle, i.e. forward scattering in the laboratory system will be preferred for titanium. In Fig. 3 one can see the functional dependency of the scattering angle in the laboratory stem with respect to the impact parameter as well as the relative probability distribution of the scattering angle θ_{LAB} in the laboratory system.

3.2 Scatter off an initially moving target

The following approach was proposed by Arnold Russek in the year 1960. His manuscript [4] is an inspiring piece of physical literature. Russek modifies the differential cross section in quite the same manner as we did in the last paragraph, i.e. the calculation of the Jacobian of the transformation from CMS into the laboratory system. But in the case of initially moving targets the Jacobian becomes very complicated. Averaging of all orientations and target speeds (with respect to a velocity distribution $f(v_t)$ he wrote[4]:

$$\sigma(\theta, T) = \int_0^\infty f(v_t) dv_t \int_0^\pi \frac{\sin\alpha}{2} d\alpha \int_0^{2\pi} \frac{1}{2\pi} \left(\frac{\sin\Theta}{\sin\theta} \left| \frac{d(\Theta, \Phi)}{d(\theta, \phi)} \right| \sigma(\Theta) \right) d\phi. \quad (33)$$

If one assumes that the targets constitute an ideal gas then the velocity distribution $f(v_t)$ is the three-dimensional Maxwell distribution. Russek derived an analytic expression for the Jacobian in terms of two parameter $\xi = v_t/v_p$ and $\eta = m_p/m_t$. But as we said before in general the integrals on the right hand side cannot be solved analytically.

Hard sphere interaction Russek [4] performed (and we checked his calculations) a Taylor expansion of the Jacobian in the case of slowly moving targets and light projectiles, i.e. $\xi \approx 0$ and $\eta \approx 0$ for elastic hard sphere scattering. The result is:

$$\begin{aligned} \frac{\sigma(T,\theta)}{R^2} &= 1 + \frac{1}{4}(3\cos(2\theta) + 1)\eta^2 + 2\cos(\theta)\eta + ... \\ &+\delta \left(\frac{1}{4}(3\cos(2\theta) + 1)\eta^3 + \frac{1}{4}(6\cos(2\theta) + 2)\eta^2 + \cos(\theta)\eta \right). \end{aligned} \quad (34)$$

Whereby we made use of the scalar $\delta := (K_B T)/E_p$. This is the differential cross section in second order. Of course the total cross section should not be affected by the relative velocity between the targets and projectiles.This can be checked by integration of Eq. 34 with respect of the scattering angles in the laboratory (θ,ϕ):

$$\sigma_{total} = \int_0^{2\pi} \int_0^\pi \sigma(T,\theta) \sin\theta d\theta d\phi = 4\pi R^2 = \pi D^2. \quad (35)$$

The associated scattering angle probability distribution is given by:

$$P(\theta, \eta, \delta) = \int_0^{2\pi} [\sigma(T, \theta) \sin\theta]\, d\phi. \tag{36}$$

In Fig. 4 one can see the scattering angle probability distribution for several projectiles at $E = 3$eV scatter off a member of an ideal gas ($T = 300$ Kelvin), which is constituted by argon atoms as well as the most probable scattering angle θ_{most} with respect to the parameter η. The scattering angle probability distribution tend to move to smaller scattering angles θ with increasing values of the mass ratio η. However, you have to keep in mind that our derived probability distribution is just valid within small values of η and small values of ζ (high projectile energy). The question arises whether we can trust our distribution for values higher than $\theta \approx 0.1$ or not? One way might be to perform exactly the same steps as before in order to derive the approximate scattering angle probability distribution but with different expansion points (say $\eta_0 = 0.3$ and $\zeta_0 = 0$) and compare the results from both expansions with each other.

The assumption of slowly moving targets is again only valid if one neglect multiple scattering of the projectile. The assumption of light projectiles is not quite satisfactory for our purpose, because we are dealing with parameter-values like $\eta \approx 0.3$;0.7 and 1.2. One approach might be to perform a Taylor expansion of the Jacobian at different values for η and ξ and try to solve as many integrals in the triple integral as possible on an analytic way. The α,ϕ,θ and ζ integration (averaging over the target velocities) are quite difficult. Within a Monte Carlo Simulation if an interaction occurs, one has to evaluate the whole four-dimensional integral to obtain the scattering angle distribution in the laboratory system. This is of course a horrible task. But to obtain highest accuracy even in high temperature regimes or the effect of thermalized sputter particles one has almost no other back door. Hence, we suggest a Monte-Carlo-Markov-Chain Method to evaluate the integrals. A detailed solution of this problem is in progress and will be the subject of future paper.

4 Monte Carlo simulations

In Fig. 5 one can see our geometry of the simulated sputter reactor.

4.1 Sputtering from targer

Sputtering from a circular planar magnetron causes the formation of a race-track in the target (see Fig. 5). The profile of the race-track is approximated by a Gauss distribution: $P(R) = \frac{1}{\sigma\sqrt{2\pi}} \exp\left(-\frac{R-\mu}{2\sigma^2}\right)$. The radius of the experimental race-track is 7.5mm (which is used for the mean μ of the gauss distribution) and the width of the race-track is 5 mm (from which the standard deviation is calculated $3\sigma = 2.5$mm).

4.2 Angular distribution

The angular distribution of out coming particles from the sputter material is modeled by a sine distribution, i.e. the relative amount of particles leaving the sputter material perpendicular to its surface ($\theta_0 = 90$) is 1. Differences in the angular distribution between the different species are not modeled but can not experimentally excluded.

4.3 Ionisition rates and ion energy distribution

The ionisation rate of sputtered particles are very low, and thus no influence on the particle distribution is assumed. But in contrast, the particle's energy seems to be of high importance. Unfortunately, until now no energy distribution for our compound target (Ti_3SiC_2) is available. In Fig. 6 one can see the ion energy distribution, which is modeled with reference to a Ti-target. One can see that most of the ions are at energies close to 3eV. In order to simulate the ion transport it is necessary to calculate the velocity of the ions.With

$$E = H = \frac{p^2}{2M} = \frac{1}{2}Mv^2$$

it follows that

$$v = \sqrt{\frac{2E}{M}}. \tag{37}$$

The energy of the ions is given in units of electron volts (eV) and the mass of the ions is given in atomic units (u). Therefore one can compute the velocity in units of cm per second by using

$$v = \sqrt{\frac{2E[eV]}{m[u]}} \cdot 9.824 \cdot 10^5 = v[cm/s]. \tag{38}$$

In two spatial dimensions, one has two velocity components. ϕ_0 is the direction angle of the ion (see angular distribution of the ions) the velocity components can be calculated by

$$v_x = v \cdot \cos(\phi_0) \tag{39}$$

$$v_y = v \cdot \sin(\phi_0) \tag{40}$$

Now, we want to apply our two interaction models to DC and high power impulse sputtering for Ti_3SiC_2. In general if several independent interaction mechanism can occur, the mean free path is not an additive quantity, but in contrast the total cross section is an additive quantity. In order to reduce the computational effort, we decided to use an event-driven Monte Carlo method in contrast to the usually used time-driven Monte Carlo method. It is therefore necessary to determine, when the next interaction will occur. If the velocity (v) and the mean free path (λ) of the particle is known, one can compute the collision frequency τ by using

$$\tau = \frac{v}{\lambda} = \frac{\sqrt{v_x^2 + v_y^2}}{\lambda}. \tag{41}$$

With the help of the collision frequency one is able to compute the time interval until the interaction occurs

$$\delta t = -\frac{\log(r)}{\tau}. \tag{42}$$

Whereby r is a random number from a uniform distribution between zero and one. Instead of simulating the trajectory of all particles in a Monte Carlo run with a fixed time step, one can use the above mentioned formula to adjust the time step. the strategy is as follows, one calculates the time interval δt for every particle (except the background particles) within a Monte Carlo run (trial), and finds the minimum value. The particle related to the minimum value of δt will first undergo an interaction. The Monte Carlo time step is set to this minimum value (event driven MC). After the time step, the specific particle will undergo the interaction, and all other particles are just move along they're specific trajectory. i.e. in the absence of any external forces the trajectory is just a straight line (this is motivated by the fact the even if external fields are set up, inside the plasma the particles will behave as if they were free, due to the electric conductance of the plasma). If an interaction with the background gas (argon) occurs, we assume a uniform impact parameter distribution in the center-of-mass-system (CMS) between the ion and the background gas. We first describe the simulations of DC sputtering thereafter the simulations concerning high power impulse magnetron sputtering. The several interaction processes can be put into an abstract interaction model (Pathway model, see [7]) that binds the interaction parameter together. A schematic drawing can bee seen in Fig. 7.

4.4 DC sputtering

In DC sputtering with low direct currents one can use the elastic hard sphere interaction to model the transport phenomena at the microscopic scale.

First experiment: only hard sphere interaction In Fig. 8 the results of 100.000 Monte Carlo events are shown, whereby we used the following experimental setup parameter:

Parameter	Value
Temperature (T)	300K
Ar-pressure (p_{Ar})	$4 \cdot 10^{-3}$mbar
S-T-distance (d)	variable from 1cm to 24cm

4.5 High power impulse magnetron sputtering

In HIPPIMS one can assume that at least a fraction of particles (sputter particles as well as target particles) are ionized. Unfortunately, there is no specific relation between pulse duration and/or pulse hight and the percentage of ionized particles. The next results are therefore very academic. In our first experiment concerning HIPPIMS we assume that all gas particles and sputter particles are simply ionized. This is of course a realistic property for the gas particles (argon) but not for the sputter particles.

Second experiment: only Coulomb interaction If one assumes all sputter particles and all gas particles being at least simple ionized, then the interaction is completely described by the Coulomb ar screened Coulomb interaction. For sake of simplicity we assume only simple ionized particles. The results from Monte Carlo simulations can be seen in Fig. 9 whereby we used the following experimental setup parameter:

Parameter	Value
Temperature (T)	300K
Ar-pressure (p_{Ar})	$4 \cdot 10^{-3}$mbar
S-T-distance (d)	variable from 1cm to 24cm

Third experiment: mixed interactions If one assumes the sputter particles consists of ionized as well as neutral atoms two interactions with the background gas can occur: hard sphere collisions if **one** of the collisions particles is neutral, and Coulomb interaction if **both** collision particles are at least simple ionized. We assumed the particles being only simple ionized and therefore we have chosen the following effective atomic numbers Z_{eff} with respect to the Slater rules in atomic physics:

atom (ionized)	electron configuration	Z_{eff}
${}_6C^+$	$(1s^2),(2s^22p^1)$	$6-2.75=3.25$
${}_{14}Si^+$	$(1s^2),(2s^22p^6)(3s^23p^1)$	$14-9.85=4.15$
${}_{22}Ti^+$	$(1s^2),(2s^22p^6),(3s^23p^63d^1),(4s^2)$	$22-19=3$
${}_{18}Ar^+$	$(1s^2),(2s^22p^6),(3s^23p^5)$	$18-11.25=6.75$

In Fig. 10 one can see the results from our simulation whereby we used the following experimental setup parameter:

Parameter	Value
Temperature (T)	300K
Ar-pressure (p_{Ar})	$4\cdot10^{-3}$mbar
S-T-distance (d)	constant 5cm
percentage of ionized carbon	30%
percentage of ionized silicon	30%
percentage of ionized titanium	30%
percentage of ionized argon	variable from 0% up to 100%

The results from the Monte Carlo simulation with several ionisation degrees of argon atoms indicates that the ionisation degree plays almost nor role for our experimental setup parameter. All results show a dominance of titanium atoms at far distances from the target axis at the substrate. The most reliable member of the stoichiometry is again silicon. One can easily see that the effect of the ionisation degree of argon atoms is suppressed due to the low ionisation degree of the sputter particles. There are several experimentally obtained indications that the ionisation degree of the sputter particles is not the assumed one, but particle dependent (electronic structure) as well as particle energy dependent. Therefore, further investigations concerning the ionisation degree of the sputtered particles as well as the argon atoms are important and will be the subject of future paper.

Link to the Pathway Model & convergence test: In the following section we want to investigate the link to the Pathway Model[7] and our Monte Carlo simulations. The most important parameter in the Pathway Model of the transport phenomena is the Loss factor. First predictions (rough estimations) can be made by inspection of the mean free paths for the sputter species. Carbon has almost the largest mean free path and therefore it will be just slightly effected by the interaction mechanism with the background gas. In Fig. 11 one can see our

results for the Loss factor of several sputter species and the different interaction models, i.e. pure hard sphere, pure Screened Coulomb and mixed interactions (described by the three experiments). One can easily see that the values for the Loss factor are almost constant after some equilibrium trials. This indicates a way to observe the **convergence** behavior of our Monte Carlo algorithm. Thus, with the help of the Loss factor we can estimate the minimum Monte Carlo trials within a simulation and conclude from the equilibrium tendency that our implementation was done correct. It is important to remember that the equilibrium MC time (number of MC trials) for Loss factor differ from Monte Carlo run to Monte Carlo run even with the same experimental setup parameter. We see that 100.000 Monte Carlo trials (events) our almost enough to equilibrate the system, i.e. reach convergence.

5 Conclusion

So far, we developed an appropriate Monte Carlo Method based on a Pathway Model for interactions between sputtered particles and a background gas, which is assumed to be an ideal gas. We set up a novel equation for the mean free path which incorporates all physical parameter like temperature and gas pressure, but most important it respects the movement of target atoms, i.e. argon particles. With the help of our theoretical investigations we performed several Monte Carlo simulation for direct current (DC) and high power impulse magnetron sputtering (HIPPIMS). The results from our simulations are qualitively in agreement with experimentally obtained stoichiometric compositions at the substrate. We were thus able to manifest that in DC sputtering the main interaction between the sputter particles and the background gas is of hard sphere type, i.e. purely geometric. In HIPPIMS a mixture of hard sphere and Coulomb interaction takes place. Unfortunately, the lack of experimentally obtained data concerning the ionisation degree of the sputtered particles and the background gas forbids a direct comparison between simulation and experiments. In future we hope to extract the ionisation degree from first principles or by data fitting to experimentally obtained results. The effect of moving targets to the differential cross section, i.e. angular distribution of sputtered particles after a collision needs an appropriate Monte-Carlo-Markov-Chain method. The energy and angular distribution of the sputter process needs also some investigations in order to achieve a one to one correspondence between simulation and experiment. Our nearest future work will dominantly deal with the energy and angular distribution at the target. We are going to use Monte Carlo simulations (TRIM software) in order to obtain a detail description of the sputter process too and incorporate these results as boundary conditions to our transport simulation.

6 Acknowledgments

This work was funded by the Federal Ministry of Education and Research under the contract number 03 SF 0325 A.
We additional thank Dipl.-Ing. Martin Balzer, FEM, Schwäbisch Gmünd, Germany for his discussions and nice inspirations to this work.

A Derivation of the mean relative velocity

Within the framework of statistical mechanics - the mean value of an observable O can be computed via

$$< O >= \frac{\int\int O(q,p) Z\,(q,p;H)\, d^{3N}q d^{3N}}{\int\int pZ\,(q,p;H)\, d^{3N}q d^{3N}}. \tag{43}$$

With q describing canonical coordinates and p canonical momenta of an N-particle-system, i.e. $H(q,p)$ obey the Hamilton equation of motion. The probability distribution Z depends on the total Hamilton function H of the system. Within the canonical ensemble one has the following relation

$$Z = \exp\left(-\frac{H(q,p)}{k_B T}\right). \tag{44}$$

With $p = mv$ and the assumption of an ideal gas the Hamilton function for the background gas is constructed only by the kinetic energies of the gas particles

$$H = \sum_{i=1}^{N} \frac{p_i^2}{2m_i}. \tag{45}$$

If $O = O(p)$ then the coordinate integration gives a volume factor in the numerator and denominator and therefor no contribution. The momentum integration can be done immediately and results in gaussian integrals. The result for the mean relative velocity is therefore given by

$$< \boldsymbol{O} = \boldsymbol{v_{rel}} >= \int\int\int_V |\boldsymbol{v_{proj}} - \boldsymbol{v_{target}}| \widetilde{Z}(\boldsymbol{v_{target}}) d\boldsymbol{v_{target}}, \tag{46}$$

with $\widetilde{Z} = (A/\pi)^{3/2} \frac{1}{2\sqrt{2}} \exp\left(-A\boldsymbol{v}^2\right)$ the reduced partitition function (Maxwell distribution) and $A = M_{target}/2k_BT$. By substituting $\boldsymbol{u} = \boldsymbol{v_{target}} - \boldsymbol{v_{proj}}$ and $d\boldsymbol{u} = \boldsymbol{v_{target}}$ one gets

$$\begin{aligned} &< |\boldsymbol{v_{rel}}| >= \int\int\int_V |u| \exp\left(-Av_{proj}^2 - 2Av_{proj}u - Au^2\right) du = \\ &= \underbrace{\frac{(A/\pi)^{3/2} \exp\left(-A{\boldsymbol{v_{proj}}}^2\right)}{2\sqrt{2}}}_{=:C(a,A)} \int\int\int_V |\boldsymbol{u}| \exp\left(-2A\boldsymbol{v_{proj}}\boldsymbol{u} - A\boldsymbol{u}^2\right) d\boldsymbol{u}. \end{aligned} \tag{47}$$

By using spherical coordinates with $r = |\boldsymbol{u}|$, $a = |\boldsymbol{v_{proj.}}|$ and $\boldsymbol{v_{proj}} \cdot \boldsymbol{u} = |\boldsymbol{v_{proj}}| \cdot |\boldsymbol{u}| \cos\theta$ one gets

$$< |\boldsymbol{v_{rel}}| > = C(a,A) \int_0^{\infty} \int_0^{2\pi} \int_0^{\pi} r \exp\left(-Ar^2 - 2A \cdot a \cdot r \cdot \cos\theta\right) r^2 \sin\theta d\theta d\phi dr$$
$$= 2\pi C(a,A) \int_0^{\infty} r^3 \int_0^{\pi} \exp\left(-Ar^2 - 2Aar\cos\theta\right) \sin\theta d\theta dr. \quad (48)$$

The double integral on the right hand side can be evaluated and its solution is given by:

$$\int_0^{\infty} r^3 \int_0^{\pi} \exp\left(-Ar^2 - 2Aar\cos\theta\right) \sin\theta d\theta dr =$$
$$\frac{\left(\frac{A}{\pi}\right)^{3/2} \exp\left(-a^2 A\right)}{2\sqrt{2}} \left(\frac{2\sqrt{A}a + \left(2Aa^2 + 1\right) \exp\left(a^2 A\right) \sqrt{\pi} \mathrm{erf}\left(a\sqrt{A}\right)}{4aA^{5/2}} \right). \quad (49)$$

After some simplification the mean relative velocity reads

$$< |\boldsymbol{v_{rel}}| >= \frac{\left(2a + \frac{1}{Aa}\right) \mathrm{erf}\left(a\sqrt{A}\right) + \frac{2\exp\left(-a^2 A\right)}{\sqrt{A}\sqrt{\pi}}}{4\sqrt{2}}. \quad (50)$$

Whereby we made use of the scalar $s := a\sqrt{A}$.
With $a = |\boldsymbol{v_{proj}}|$ the final result for the mean relative velocity between projectiles probing into a mono atomic ideal gas is given by

$$< |\boldsymbol{v_{rel}}| >= \frac{\left[\left(s + \frac{1}{2s}\right) \mathrm{erf}(s) + \frac{1}{\sqrt{\pi}} \exp\left(-s^2\right)\right]}{3s} \times |\boldsymbol{v_{proj}}|. \quad (51)$$

q.e.d.

References

1. P. Eklund, M. Beckers, J. Frodelius, H. Högberg, and L. Hultman. *Magnetron sputtering of Ti3SiC2 thin films from a compound target.* JVST A, 25(5):1381-1388, 2007.
2. P. Eklund. *Multifunctional nanostructured Ti-Si-C thin films.* Linköping studies in science and technology, Dissertation No. 1087, 2007
3. H. Goldstein. *Classical Mechanics.* Addison-Wesley Series in Physics, Second edition (1980).
4. A. Russek. *Effect of Target Gas Temperature on the Scattering cross section.* Phys. Rev. 120, 1536 - 1542 (1960).
5. S. Mahiheu, G. Buyle, D. Depla, S. Heirwegh, P. Ghekiere, R. De Gryse. *Monte Carlo simulation of the transport of atoms in DC magnetron sputtering.* Nuclear Instruments and Methods in Physics Research B 243:313-319, 2006.
6. E. Everhart, G. Stone, R. J. Carbone. *Classical Calculation of Differential cross section for Scattering from a Coulomb Potential with Exponential Screening.* Phys. Rev. Vol. 99,Number 4:1287-1290, 1955.
7. D.J. Christie. *Target material pathways model for high power pulsed magnetron sputtering.* J.Vac.Sci. Technology, 23:2, 330-335, 2005.

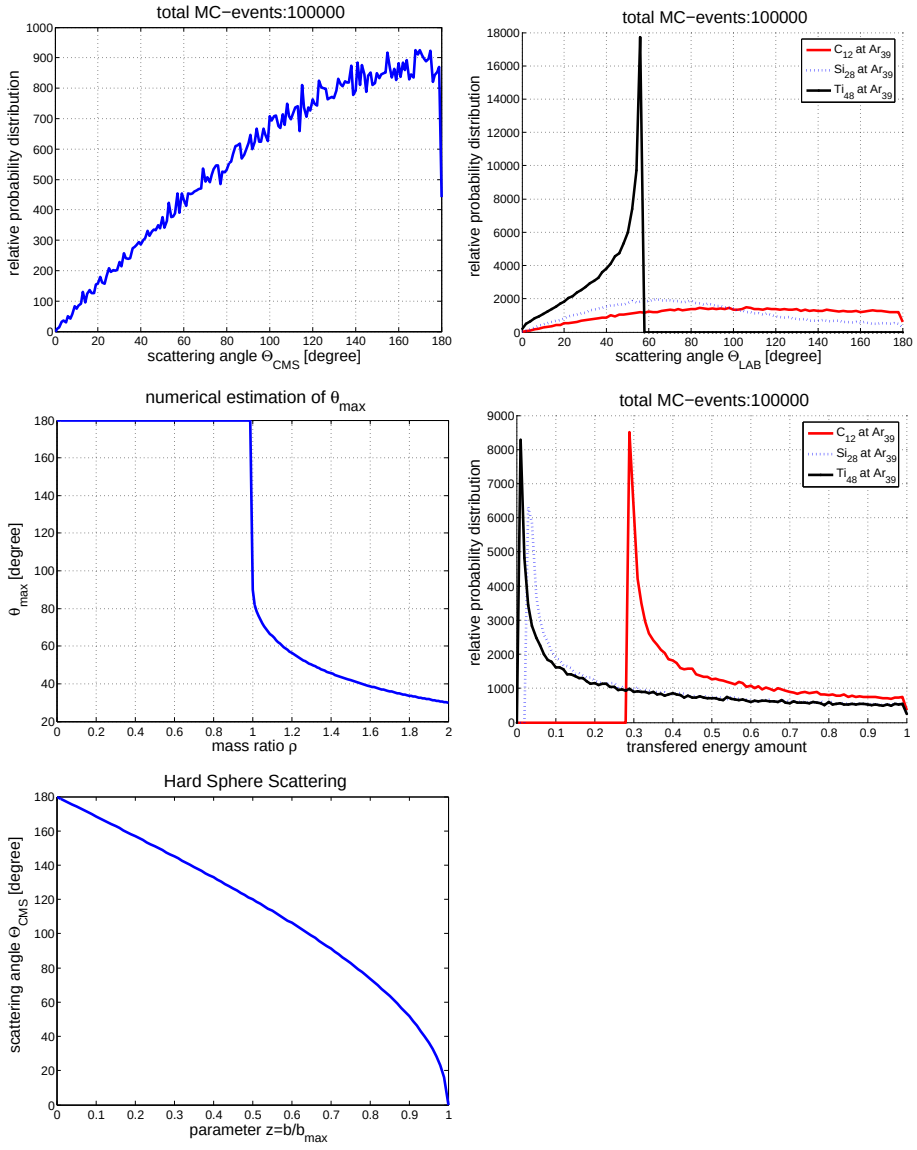

Fig. 2. Results from one hard sphere collision (initially resting targets). **Upper left:** scattering angle distribution of Θ_{CMS} in the CMS system and **upper right:** Monte Carlo results of the scattering angle probability distribution in the laboratory system. **Middle left:** numerical determination of the maximal scattering angle θ_{max} in the laboratory and **Middle right:** probability distribution of the transfered energy via Monte-Carlo Simulations. **Lower left:** scattering angle Θ_{CMS} with respect to the scattering parameter z.

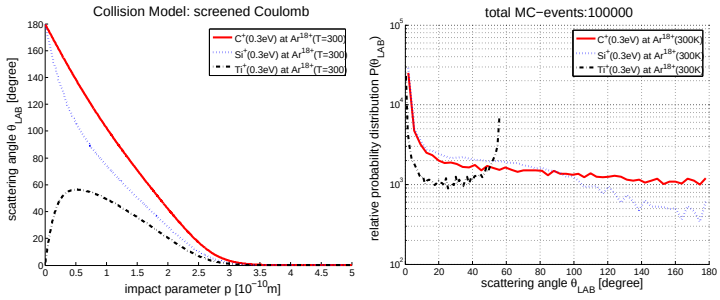

Fig. 3. Results from the screened Coulomb collision model under the assumption of fully ionized argon gas particles and simple ionized projectile particles.
left: scattering angle θ_{LAB} with respect to the impact parameter and **right:** the relative scattering angle distribution of Θ_{LAB}.

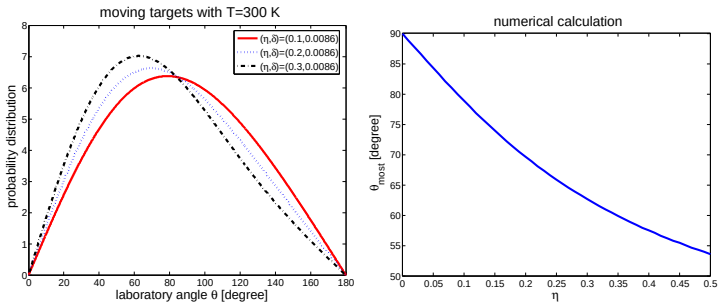

Fig. 4. Results for hard sphere interaction with respect to moving targets (Eq. 34)
left: scattering angle probability distribution for several projectiles at argon targets and **right:** numerical determination of the most probable scattering angle θ_{most}. One can easily see that even in the case of heavy projectiles all scattering angles are possible in contrast to the angle distribution with initially resting targets.

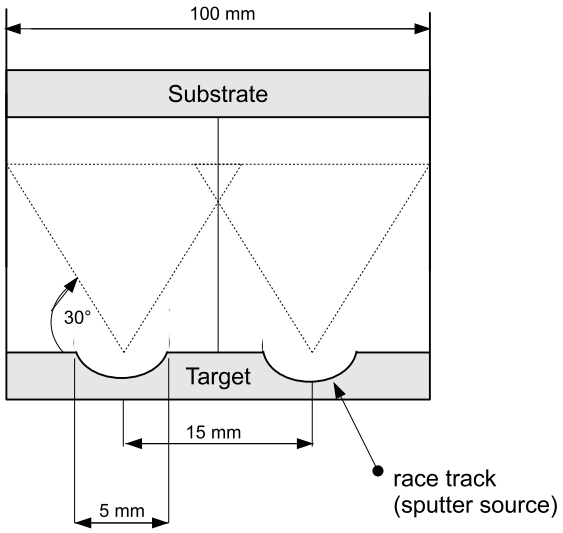

Fig. 5. Our chosen geometry of the simulated sputter reactor.

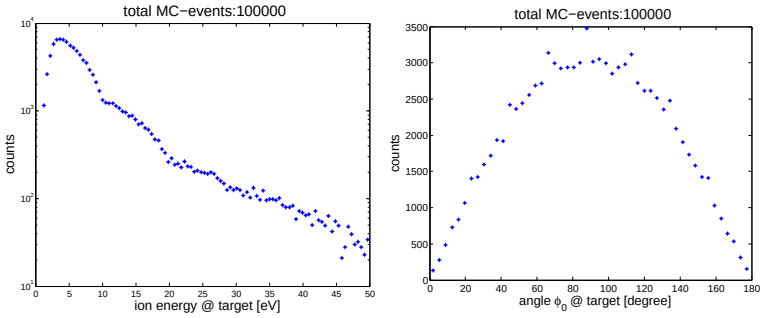

Fig. 6. Assumed energy and angular distribution of the sputtered species at the target. One can see that most of the sputter particles have energies around $3 - 5$ eV. The angular distribution is a transformed cosine transformation (this is justified by the assumption that the sputter process can be described by elastic hard sphere interaction between argon atoms and particles within the sputter compound target).

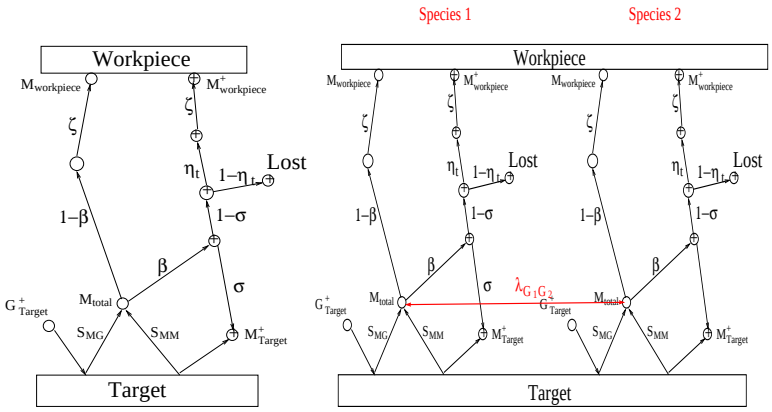

Fig. 7. left: Single Pathway model and **right:** Multi Pathway model (Christie 2005).

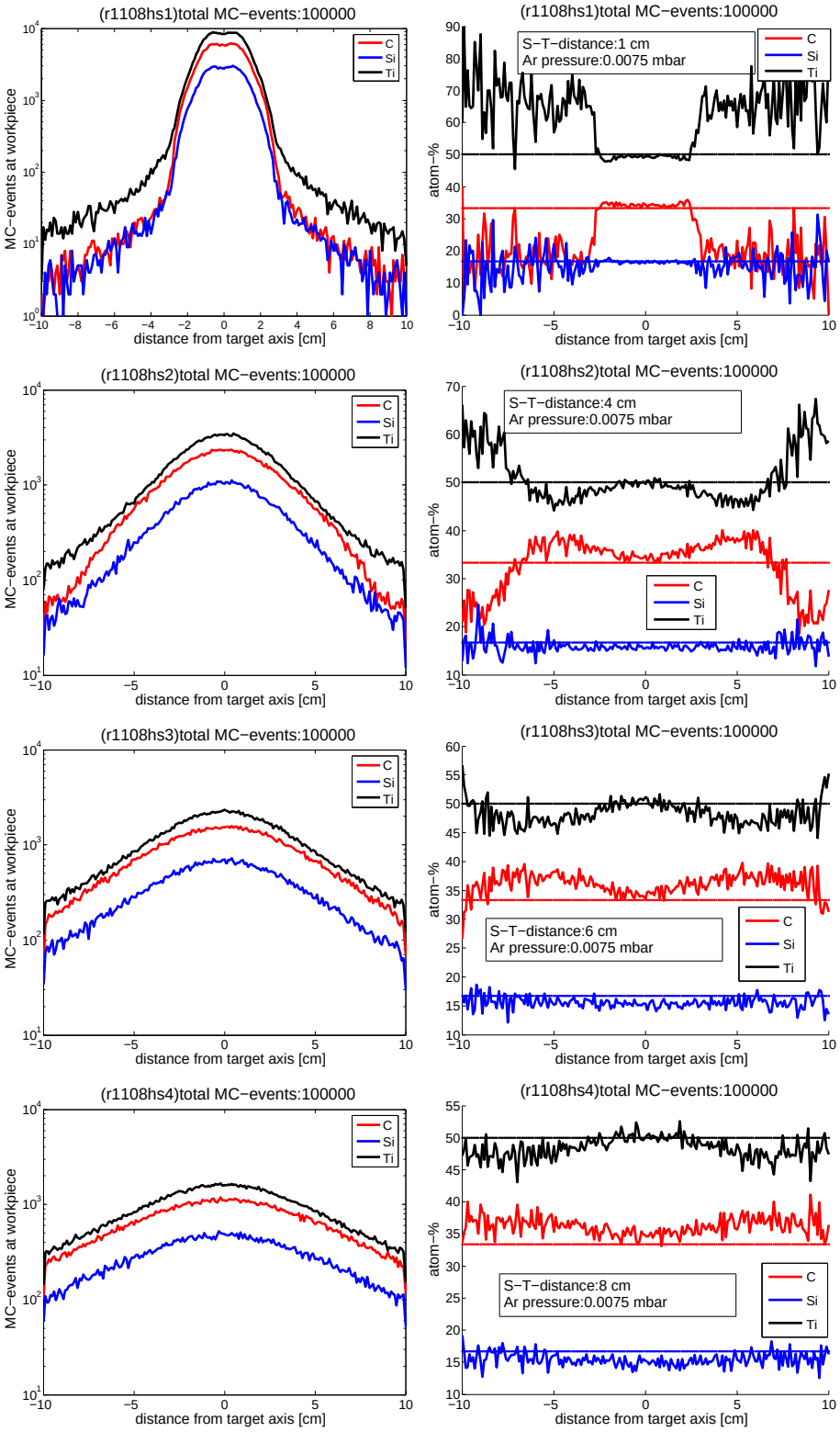

Fig. 8. Results from the first experiment:
left: registered Monte Carlo events at the workpiece and **right:** stoichiometric composition at the workpiece for several target-substrate-distances in cm whereby we assumed a pure hard sphere interaction between the sputter particles and the gas particles.

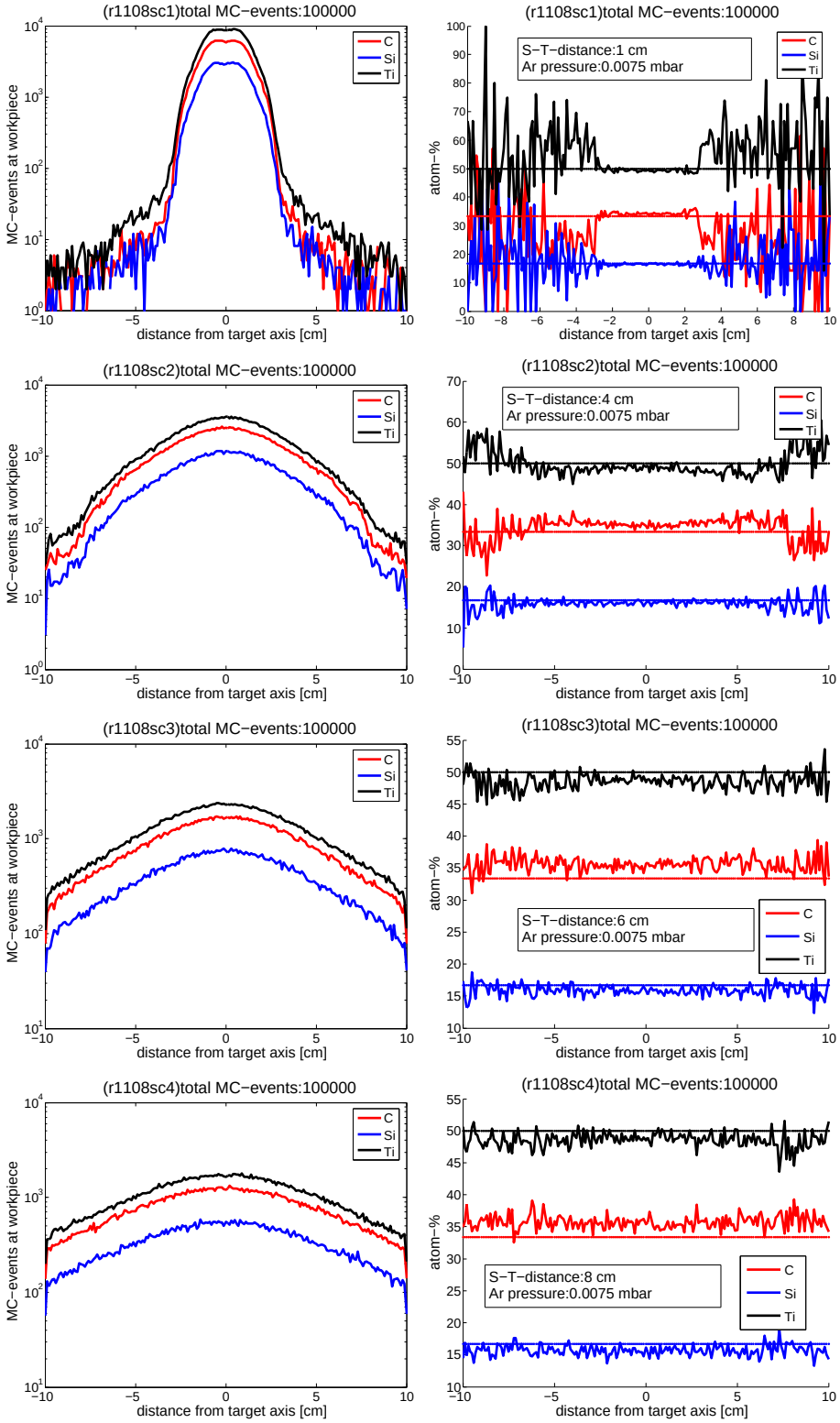

Fig. 9. Results from the second experiment:
left: registered Monte Carlo events at the workpiece and **right:** stoichiometric composition at the workpiece for several target-substrate-distances in cm whereby we assumed a pure Coulomb interaction between the sputter particles and the gas particles (simple ionized species).

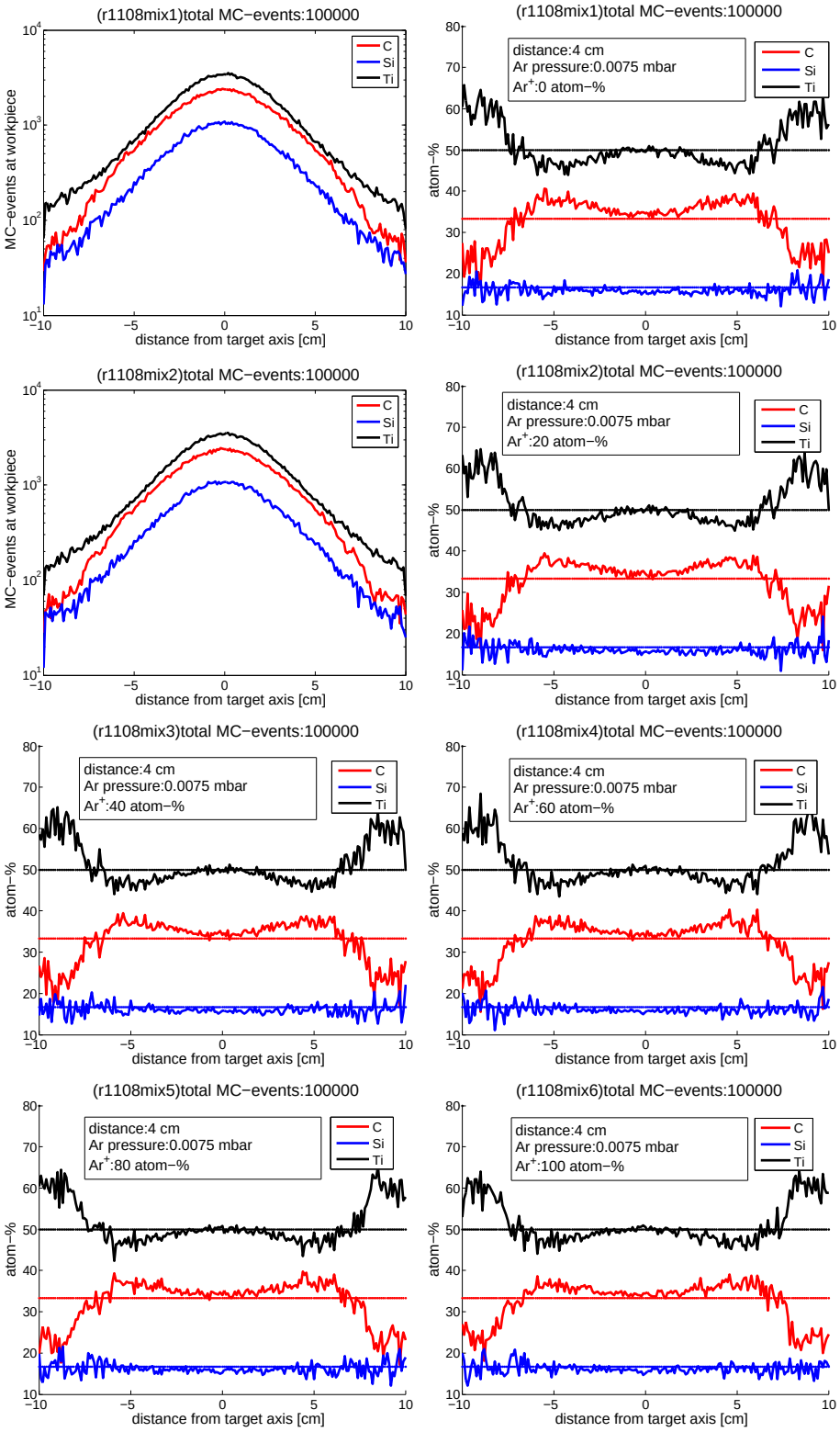

Fig. 10. Results from the third experiment:
left: registered Monte Carlo events at the workpiece and **right:** stoichiometric composition at the workpiece for several ionization degrees of argon whereby we respected mixed interactions between the sputter particles and the gas particles (simple ionized species).

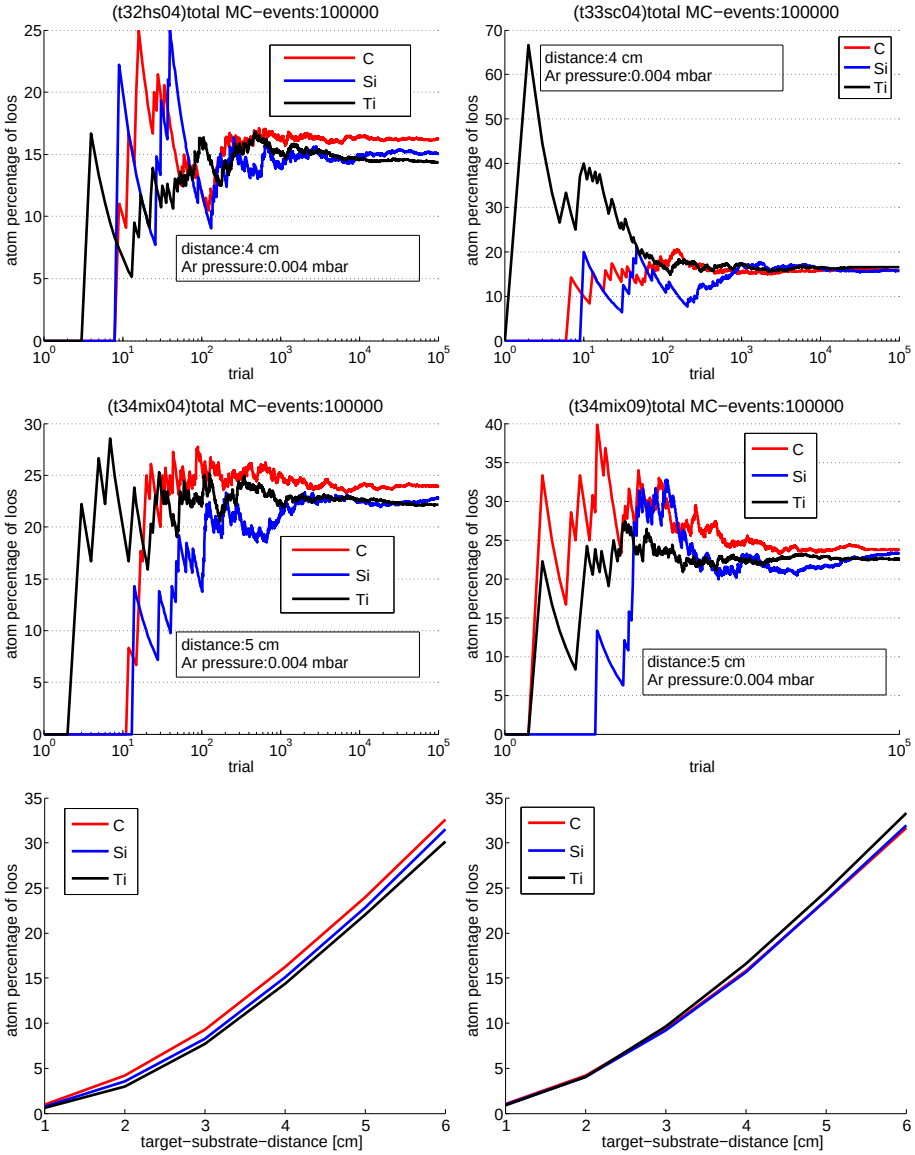

Fig. 11. Link to the Pathway-Model (Loss factor):
top left: Loss factor for pure hard sphere interaction and **top right:** for pure Coulomb (screened) interaction between the sputter species and the background gas. **middle left:** Loss factor for a mixed interaction (40% ionisation of argon atoms and 10% ionisation of the sputter atoms) and **middle right:** Loss factor for a mixed interaction with 90% ionisation of argon atoms. **bottom left:** Loss factor for pure hard sphere interaction (DC sputtering) with respect to the target-substrate-distance. **bottom right:** Loss factor for pure Coulomb interaction with respect to the target-substrate-distance.